

## Supporting Information

### Hexagonal boron nitride inducing anionic trapping in polyethylene oxide based solid polymer electrolyte for lithium dendrite inhibition

Yuhan Li,<sup>a</sup> Libo Zhang,<sup>a</sup> Zongjie Sun,<sup>a</sup> Guoxin Gao,<sup>a\*</sup> Shiyao Lu,<sup>a</sup> Min Zhu,<sup>a</sup> Yanfeng Zhang,<sup>a</sup> Zhiyu Jia,<sup>b</sup> Chunhui Xiao,<sup>a</sup> Huaitian Bu,<sup>c</sup> Kai Xi,<sup>d</sup> Shujiang Ding<sup>a\*</sup>

<sup>a</sup> Department of Applied Chemistry, School of Science, Xi'an Key Laboratory of Sustainable Energy Materials Chemistry, MOE Key Laboratory for Nonequilibrium Synthesis and Modulation of Condensed Matter, State Key Laboratory of Electrical Insulation and Power Equipment, Xi'an Jiaotong University, Xi'an 710049, China.

<sup>b</sup> MOE Key Laboratory of Cluster Science, School of Chemistry and Chemical Engineering, Beijing Institute of Technology, Beijing 100081, China.

<sup>c</sup> Department of Materials and Nanotechnology, SINTEF Industry, Forskningsveien 1, 0373 Oslo, Norway.

<sup>d</sup> University of Cambridge, Department of Materials Science and Metallurgy.

Email: [gaoguoxin@mail.xjtu.edu.cn](mailto:gaoguoxin@mail.xjtu.edu.cn); [dingsj@mail.xjtu.edu.cn](mailto:dingsj@mail.xjtu.edu.cn)

Keywords: Hexagonal boron nitride, polymer solid electrolyte, ion transport mechanism, Li dendrites inhibition, DFT and MD.

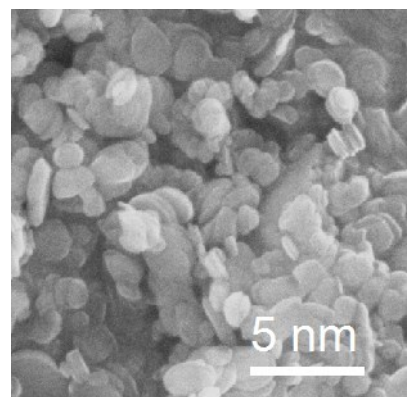


**Fig. S1** The SEM image of h-BN nanosheets.

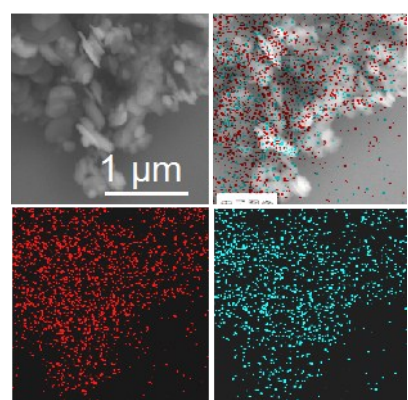


**Fig. S2** Elemental mapping images of h-BN nanosheets.

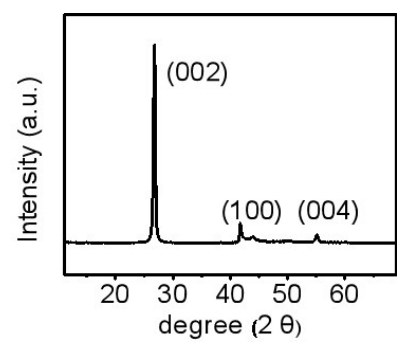


**Fig. S3** XRD spectra of h-BN.

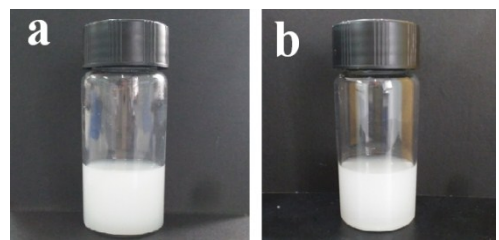


**Fig. S4** (a) Photograph of h-BN nanosheets dissolving in acetonitrile. (b) The picture of the homogeneous electrolyte solution of h-BN, PEO and LiTFSI in acetonitrile.

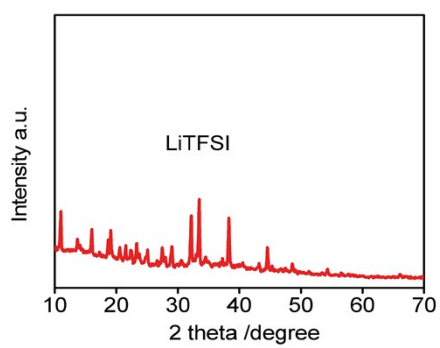


**Fig. S5** XRD of LiTFSI. The peaks at  $11.04^\circ$ ,  $16.03^\circ$ ,  $19.09^\circ$ ,  $20.55^\circ$ ,  $21.54^\circ$ ,  $23.32^\circ$ ,  $25.07^\circ$ ,  $27.4^\circ$ ,  $29.03^\circ$ ,  $32.20^\circ$ ,  $33.48^\circ$ ,  $38.30^\circ$  and  $44.54^\circ$  perfectly match to (002), (011), (201), (111), (202), (013), (113), (212), (114), (015), (115), (116) and (125) crystal planes.

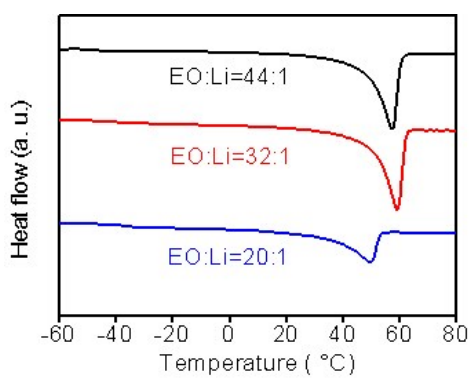


**Fig. S6** The  $T_m$  of PEO/LiTFSI/6%-h-BN with different EO: Li = 20, 32, 44.

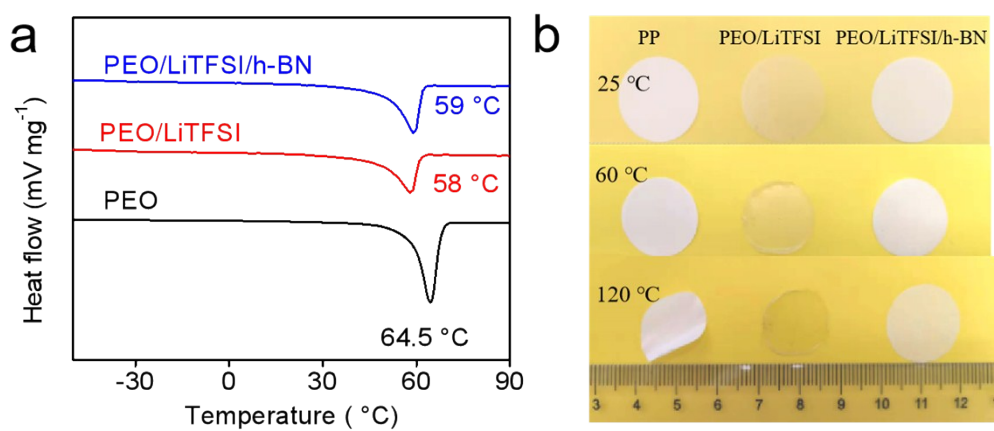


**Fig. S7** (a) The  $T_m$  of PEO, PEO/LiTFSI and PEO/LiTFSI/ $x$ =h-BN ( $x=3\%$ ,  $6\%$  and  $9\%$ ) CPE. (b) Fourier-transform infrared spectra (FTIR) of h-BN, PEO, PEO/LiTFSI and PEO/LiTFSI/ $x$ =h-BN ( $x=3\%$ ,  $6\%$  and  $9\%$ ) CPE.

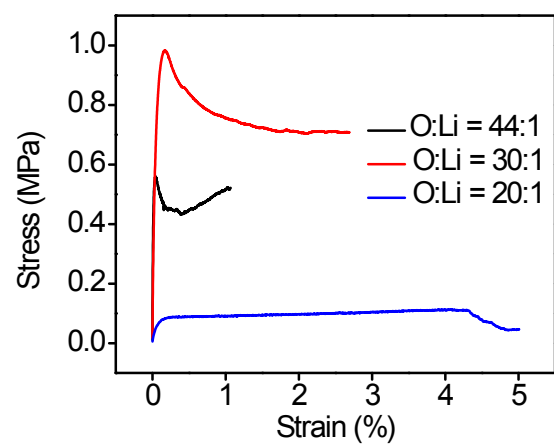


**Fig. S8** The stress-strain curves of PEO/LiTFSI/6% h-BN with different EO: Li = 20:1, 32:1, 44:1.

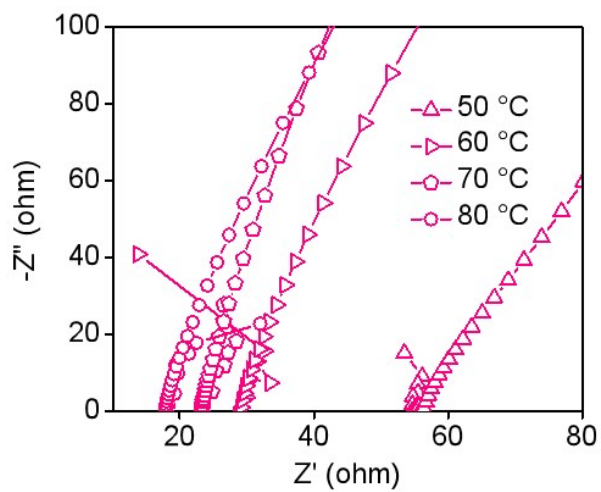


**Fig. S9** The EIS plots for PEO/LiTFSI SPE under 50-80 °C.

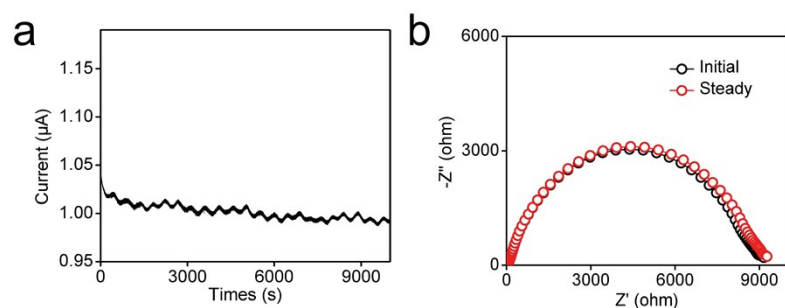


**Fig. S10** (a) I-t curve for PEO/LiTFSI SPE at 60 °C with polarization voltage of 10 mV. (b) The A.C impedance plots before and after the polarization.

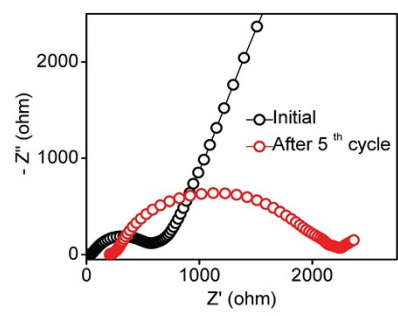


**Fig. S11** Impedance spectra of the Li/PEO/LiTFSI SPE/LiFePO<sub>4</sub> cell before and after 5 cycles at 60 °C.

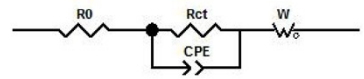


**Fig. S12** The equivalent circuit of Li/PEO/LiTFSI SPE/LiFePO<sub>4</sub> and Li/PEO/LiTFSI/h-BN CPE/LiFePO<sub>4</sub> cell at 60 °C.

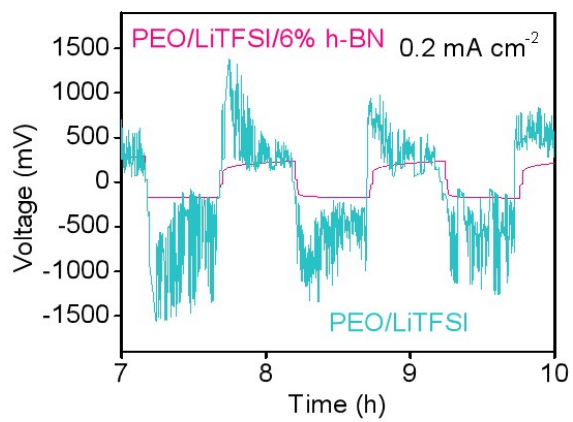


**Fig. S13** The magnified cycling curves of battery using PEO/LiTFSI/h-BN CPE and PEO/LiTFSI SPE for selected cycles.

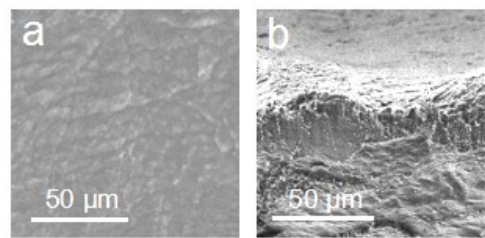


**Fig. S14** The SEM image (a) and cross-sectional image (b) of Li foil before cycle.

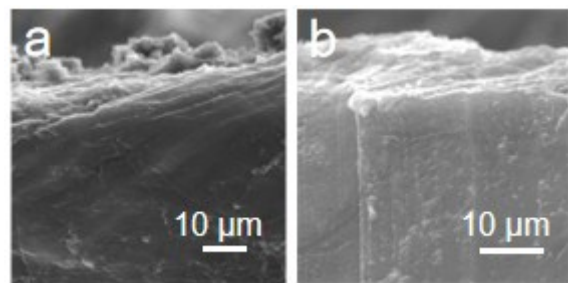


**Fig. S15** The SEM and cross-sectional image of Li anode after cycle in the batteries using PEO/LiTFSI SPE (a) and PEO/LiTFSI/6% h-BN CPE (b).



**Fig. S16** Open circuit voltage of the assembled solid-state soft-package lithium metal battery at room temperature.

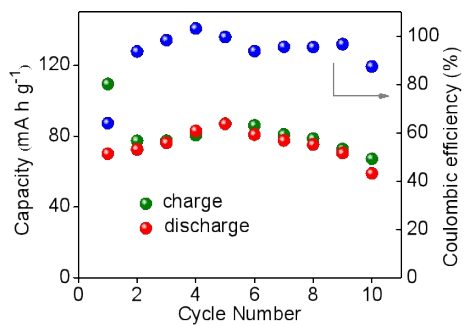


**Fig. S17** Cycle performance of Li/PEO/LiTFSI/6% h-BN/LiFePO<sub>4</sub> soft-package lithium metal battery at 0.1 C and 60 °C.

**Table S1.** The ionic conductivity of PEO/LiTFSI SPE with different contents of h-BN at different temperature.

$\sigma \times 10^{-4} \text{ S cm}^{-1}$	PEO/LiTFSI	PEO/LiTFSI/3% h-BN	PEO/LiTFSI/6% h-BN	PEO/LiTFSI/9% h-BN
303 K	0.077	0.046	0.077	0.026
313 K	0.204	0.125	0.191	0.042
323 K	0.540	0.319	0.470	0.098
333 K	0.941	0.358	0.890	0.509
343 K	1.47	0.608	1.11	0.623
353 K	2.20	0.725	1.45	0.829

**Table S2.** The ionic conductivity of PEO/LiTFSI/6%-h-BN with different OE:Li at different temperature.

$\sigma \times 10^{-4} \text{ S cm}^{-1}$	PEO/LiTFSI/6%-h-BN		
	EO:Li=20:1	EO:Li=32:1	EO:Li=44:1
303 K	0.137	0.077	0.027
313 K	0.569	0.191	0.055
323 K	1.257	0.470	0.155
333 K	1.348	0.890	0.621
343 K	1.510	1.11	0.762
353 K	1.520	1.45	0.929

**Table S3.** Comparison of electrochemical cycle performance of Li/PEO/LiTFSI/h-BN CPE/LiFePO<sub>4</sub> with other reported PEO-based electrolyte.

Electrolyte	Cycle number	Discharge capacity (cathode material: LiFePO <sub>4</sub> )	Temperature	Reference
PEO/LiTFSI/h-BN CPE	140	143 mAh g <sup>-1</sup> / 0.2 C	60 °C	This work
Ionic liquid-PEO solid electrolyte	50	140 mAh g <sup>-1</sup> / 0.1 C	60 °C	<i>J. Hydrogen Energy</i> <b>2017</b> , <i>42</i> , 7212.
PIL-IL-SiO <sub>2</sub> nanoplates PEO polymer electrolyte	30	145.5 mAh g <sup>-1</sup> / 0.1 C	60 °C	<i>Nano Energy</i> , <b>2017</b> , <i>33</i> , 110. <i>Adv. Mater.</i>
PEG-based polymer electrolyte	20	140 mAh g <sup>-1</sup> / 0.2 C	30 °C	<i>Interfaces</i> <b>2018</b> , 1801445
PEG-to-PVP triblock gel polymer electrolytes	30	135 mAh g <sup>-1</sup> / 0.1 C	60 °C	<i>Polym. Chem.</i> <b>2018</b> , <i>9</i> , 5190
Carbon quantum dots-PEO solid electrolyte	100	100 mAh g <sup>-1</sup> / 1 C	60 °C	<i>Adv. Sci.</i> <b>2018</b> , 1700996
pyrrolidone-PEO solid electrolyte	--	--	--	<i>Electrochimica Acta</i> <b>2019</b> , <i>293</i> , 25.

**Table S4.** The corresponding simulated impedance parameters in an equivalent circuit.

Battery sample	Before cycle		After 5 cycles	
	$R_b$ ( $\Omega$ )	$R_{ct}$ ( $\Omega$ )	$R_b$ ( $\Omega$ )	$R_{ct}$ ( $\Omega$ )
PEO/LiTFSI/6% h-BN	20.94	83.34	30.69	433.8
PEO/LiTFSI	37.89	447.2	178.2	1651